# Liquefaction Hazard Mapping with LPI in the Greater Oakland, California, Area

**Thomas L. Holzer,[a)] M.EERI, Michael J. Bennett,[a)] Thomas E. Noce,[a)] Amy C. Padovani,[b)] and John C. Tinsley III[a)]**

Cumulative frequency distributions of the liquefaction potential index (LPI) of surficial geologic units were used to define the liquefaction hazard in a 140-km$^2$ area along the eastern shore of San Francisco Bay near Oakland, California. LPI values were computed for 202 cone penetration tests conducted in surficial geologic units in the study area. The hazard of each unit was defined by the cumulative frequency at LPI=5. The distributions predict that 73% and 3%, respectively, of the area underlain by artificial fill and Holocene alluvial fan deposits will show surface manifestations of liquefaction during a M7.1 earthquake on the nearby Hayward Fault. The predictions are consistent with recent earthquakes in other areas where similar types of deposits experienced near-field ground motion.
[DOI: 10.1193/1.2218591]

## INTRODUCTION

Liquefaction hazard maps increasingly are being incorporated into earthquake risk mitigation practice. These maps initially resulted from research efforts by engineering geologists and geotechnical engineers and their application by communities was voluntary (Power and Holzer 1996). As the mapping methodology has matured, however, maps have been incorporated into seismic safety plans of communities and recently have been adopted in California for regulatory purposes (CDMG 1997). Because these maps typically portray the hazard within large areas, their efficient production requires that they be based on maps of surficial geology. A significant challenge in the conversion of geologic maps to hazard maps has been the assessment of the hazard posed by each geologic unit. Qualitative rankings are typically used (e.g., Youd and Hoose 1977). While standard penetration test blow counts may be collected and applied to evaluate relative liquefaction potential, the hazard posed by mapped surficial geologic units commonly is specified in descriptive terms ranging from low to very high (Power and Holzer 1996). These rankings also typically do not characterize the potential for damage.

A parameter that predicts the liquefaction potential of a geologic unit would improve liquefaction hazard mapping. If the parameter could be computed from field data and incorporated into a geographic information system (GIS), it would enhance the application of GIS technology in the preparation of hazard maps. The liquefaction potential index (LPI) has been proposed as such a parameter (Luna and Frost 1998). LPI, which was

[a)] U. S. Geological Survey, MS977, 345 Middlefield Road, Menlo Park, CA 94025
[b)] GeoSyntec Consultants, 475 14th St., Suite 450, Oakland, CA 94612


*Earthquake Spectra,* Volume 22, No. 3, pages 693–708, August 2006; © 2006, Earthquake Engineering Research Institute

originally defined by Iwasaki et al. (1978), evaluates the liquefaction potential of the soil profile to a depth of 20 m at a specific location and provides an estimate of the severity of liquefaction. However, it is the potential capability of LPI to describe the spatial variability of liquefaction hazard that makes it attractive for regional investigations and application in GIS (Crespanelli et al. 1999, Divakarla et al. 1998, Frost et al. 1997, Holzer et al. 2002, Hosseini 1998, Luna and Frost 1998, Sonmez 2003, Ulusay and Kuru 2004). This paper describes the application of LPI to quantify the liquefaction potential of geologic units for hazard mapping along the eastern shore of San Francisco Bay, California, near and including the city of Oakland. Such quantification permits local communities and other users of hazard maps to assess better the liquefaction hazard when making land use decisions and reviewing investigations in regulatory seismic hazard zones (http://www.consrv.ca.gov/cgs)

## LPI

LPI was originally proposed to estimate the potential for liquefaction to cause foundation damage (Iwasaki et al. 1978). The index weighs factors of safety and thickness of potentially liquefiable layers according to depth. It assumes that the severity of liquefaction is proportional to (1) thickness of the liquefied layer; (2) proximity of the liquefied layer to the surface; and (3) amount by which the factor of safety (FS) is less than 1.0, where FS is the ratio of soil capacity to resist liquefaction to seismic demand imposed by the earthquake.

LPI is defined as

$$LPI = \int_0^{20m} Fw(z)dz \tag{1}$$

where

$$F = 1 - FS \quad \text{for } FS \leq 1 \tag{2a}$$

$$F = 0 \quad \text{for } FS > 1 \tag{2b}$$

$$w(z) = 10 - 0.5z, \quad \text{where } z \text{ is the depth in meters.} \tag{2c}$$

The weighting factor, $w(z)$, proposed by Iwasaki et al. (1978) ranges from one at the surface to zero at 20 m. FS as defined by Iwasaki et al. (1982) explicitly considered blow counts from standard penetration tests (SPT) and median grain size when computing the liquefaction resistance. For the present investigation, we used the FS as defined in the Seed-Idriss simplified procedure (Seed and Idriss 1971, Seed et al. 1985, Youd et al. 2001) as modified for the cone penetration test (CPT) by Robertson and Wride (1997). Note that with the simplified procedure, soil above the water table is not evaluated.

LPI as applied here relies on the simplified procedure to estimate FS. The prediction by LPI, however, is more comprehensive than that made by the simplified procedure. LPI considers the liquefaction potential of the whole soil column to a depth of 20 m,

whereas the simplified procedure predicts the liquefaction potential of only a soil element. By combining all factors of safety from a single CPT sounding into a single value for the entire soil column, LPI provides spatially distributed values that are useful for regional evaluations of liquefaction potential.

The significance of LPI values has been evaluated by Iwasaki et al. (1982) and Toprak and Holzer (2003), who independently correlated LPI with liquefaction effects. Both evaluations compiled case histories that compared LPI with observed severity of liquefaction. Iwasaki et al. (1982) concluded on the basis of SPT blow counts at liquefaction sites in Japan that severe liquefaction is likely at sites with $LPI > 15$ and that severe liquefaction is unlikely at sites with $LPI < 5$. Toprak and Holzer (2003) computed LPI values from CPT soundings at sites with surface manifestations of liquefaction during the 1989 Loma Prieta, California, earthquake, and concluded that sand boils typically occurred at soundings where $LPI \geq 5$ and that lateral spreads typically occurred where $LPI \geq 12$. Their thresholds are based on median LPI values. Lower and upper quartiles were 3 and 10 for sand boils and 5 and 17 for lateral spreads. LPI in their investigation used the same definition of factor of safety and data analysis as was used in the present investigation. Use of $LPI \geq 5$ as a threshold value for the surface manifestations of liquefaction was recently supported in an investigation of liquefaction in Oceano in central coastal California, following the 2003 M6.5 San Simeon earthquake (Holzer et al. 2004, 2005b).

## ENGINEERING GEOLOGY

The study area includes the cities of Alameda, Berkeley, Emeryville, Oakland, and Piedmont along the coastal plain adjacent to San Francisco Bay in Northern California. The surficial geology of the 140-$km^2$ area is shown in Figure 1. The area contains five major surficial geologic units in addition to bedrock: artificial fill, younger San Francisco bay mud, Holocene alluvial fan deposits, Merritt Sand, and Pleistocene alluvial fan deposits. Unified Soil Classification System types and approximate geologic ages of the surficial geologic units are shown in Table 1. The study area can be subdivided into three broad northwest-southeast-trending regions on the basis of surficial geology. The area southwest of the original natural shoreline—the landward extent of artificial fill—is primarily underlain by artificial fill that rests on younger San Francisco Bay mud. Immediately northeast of the natural shoreline is the central area where the surficial geology consists of Holocene and Pleistocene alluvial fan deposits. Northeast of the central area, bedrock is exposed at the land surface.

The sandy artificial fills in the western area were emplaced both by hydraulic dredging and placement from land before 1964. Most of the fill was emplaced without consideration for its vulnerability to liquefaction, although soils have been improved at some sites. Fill thickness as penetrated by CPT soundings ranges from about 11 m to zero, where the fill pinches out along the original shoreline. Average thickness is about 3 m. The Holocene alluvial fan deposits in the central area generally consist of fine-grained deposits, although fluvial sands locally are present. Thickness of the fan deposits as penetrated by CPT soundings ranges from about 14.3 m to zero where they overlap deposits of Pleistocene age. Average thickness is about 4.4 m. The fan complex was ac-

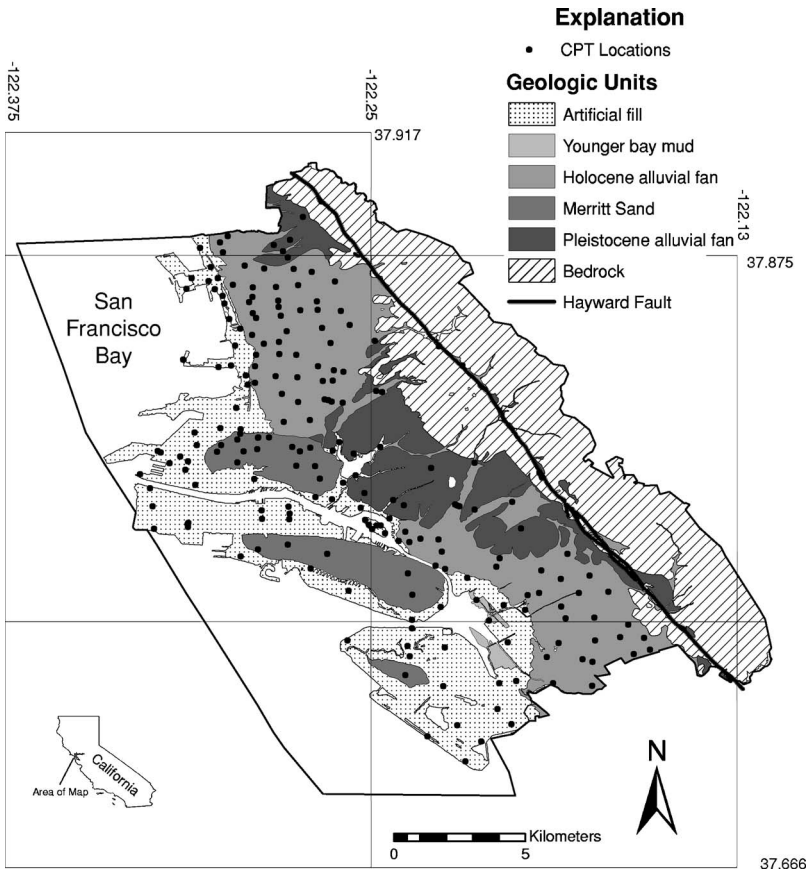


**Figure 1.** Generalized map of surficial geology of Alameda, Berkeley, Emeryville, Oakland, and Piedmont, California (modified from Halley and Graymer, 1997).

**Table 1.** Unified Soil Classification System (USCS) and estimated ages of geologic units (Holzer et al. 2005a)

| Geologic Unit | USCS Soil Type | Geologic age (years) |
|---|---|---|
| Artificial fill | SM | Modern |
| Younger bay mud | CL | Holocene (<8,000) |
| Holocene alluvial fan | CL, SM | Holocene (<15,000) |
| Merritt Sand | SM | Pleistocene (80,000–10,000) |
| Pleistocene alluvial fan | CL, SM | Pleistocene (>116,000) |

tive until modern urban development covered the land surface and channelized the modern streams (Sowers 1993). These fan deposits rest on older Pleistocene alluvial fan deposits that were last active during the previous interglacial period (Trask and Rolston 1951). The upper surface of the Pleistocene alluvial fan deposits is heavily dissected as the result of tectonic uplift and stream incision. The latter was caused by both lowering of stream base level when sea level declined during the last major continental glaciation and a wetter climate. The Merritt Sand, which is predominantly a wind-blown deposit, locally overlies the Pleistocene alluvial fan deposits. The Merritt Sand was chiefly deposited during and near the end of the Pleistocene epoch when sea level was below its current level. Ground water is presently encountered at less than 3 m depth in much of the study area.

The Hayward Fault is the most important seismic source in the study area on the basis of its location and activity (Figure 1). Investigators of earthquake recurrence on the Hayward/Rodgers Creek Fault system predict a probability of 0.27 of a $M \geq 6.7$ earthquake in the period 2002–2031, where M is moment magnitude (WGCEP 2003). In a preliminary report (WGCEP 1999), which was what was available at the time of this study, these investigators estimated a rupture of both north and south segments of the Hayward Fault would produce a M7.1 earthquake. Rupture of only the northern segment, which is in the study area, was estimated to cause a M6.6 earthquake. The last damaging earthquake on the Hayward Fault was an estimated M6.8 in 1868 when the southern segment ruptured (WGCEP 2003).

## METHODOLOGY

A total of 202 seismic CPT soundings were conducted in the study area to enable computation of LPI values in artificial fill and Holocene and Pleistocene surficial geologic units (see locations in Figure 1). In addition to measuring penetration resistance, shear-wave velocity ($V_S$) was measured in each sounding. $V_S$ was used both to help identify geologic units in soundings and to prepare maps of NEHRP site classes based on 30-m-average velocity ($V_{S30}$) (Holzer et al. 2005a, c). Seismic CPT data are available at http://quake.usgs.gov/prepare/cpt/. Although some commercial standard penetration test data were available, their quality was highly variable. In addition, penetration data in individual borings typically were incomplete. Thus the borings did not materially improve the characterization of the spatial variability of LPI as indicated by the CPT soundings and were not used in this investigation to compute LPI.

For classification of soil type with the CPT, we used the soil behavior type index ($I_C$) described by Robertson (1990). $I_C$ predicts soil class from normalized values of tip resistance and friction ratio. $I_C$ values are used by Robertson and Wride (1997): (1) to test if an interval penetrated by the CPT is susceptible to liquefaction and warrants computation of its liquefaction potential, and (2) to obtain clean sand equivalent CPT penetration resistance. Although we relied on $I_C$ to infer liquefaction susceptibility, spot sampling in holes adjacent to selected CPT soundings was conducted to confirm that soil types were classified properly with regard to their liquefaction susceptibility. A total of 113 soil samples from 27 soundings were analyzed. The principal issue that prompted the sampling involved soils with $I_C$ values around 2.60. We found that some soils with $I_C$

around 2.60 were misclassified as liquefiable sand mixtures (silty sand to sandy silt) because measured CPT penetration resistance indicated $I_C < 2.60$. The soils were actually silt mixtures (clayey silt to silty clay), i.e., $I_C$ should have been greater than 2.60. Clay contents of samples of the misclassified soils were greater than 15%, which indicates they should not be susceptible to liquefaction. Most of these misclassifications occurred in strongly weathered Pleistocene alluvial fan deposits. Accordingly, we typically sampled intervals where we encountered Pleistocene alluvial fan deposits with $I_C$ around 2.60 and that were predicted to be susceptible to liquefaction. We recognize that the liquefaction criteria of the simplified procedure continue to evolve (e.g., Cetin et al. 2004), but the criteria for this study were appropriate for the time it was conducted.

LPI values were computed for each CPT sounding based on M6.6 and 7.1 earthquakes on the nearby Hayward Fault. Constant peak horizontal ground accelerations (PGA) of 0.4 and 0.5 g, respectively, were used at each sounding to compute the factors of safety required for calculation of the LPI for the M6.6 and 7.1 earthquakes. PGA values were estimated with the ground motion prediction equation of Boore et al. (1997) and are based on average distance of the study area from the fault and average soil conditions. The assumption of a constant PGA was justified on the basis that the outcrop area of each surficial unit generally parallels and is close to the Hayward Fault. Thus most of the study area can be expected to experience large ground motions (PGA $\geq 0.4$ g) during a Hayward Fault earthquake. Because predictions of liquefaction potential by the Seed-Idriss simplified procedure for a given earthquake magnitude do not vary greatly for PGA $\geq 0.4$ g, variations in ground motion above this level will have a modest impact on LPI. This is because the liquefaction resistance boundary at PGA $\approx 0.4$ g reaches a vertical asymptote at a corrected CPT tip resistance ($q_{c1N}$) of approximately 160 (e.g., see Youd et al., 2001; Figure 4). Accordingly, most of the sand with $q_{c1N} < 160$ is predicted to liquefy, and sand with $q_{c1N} > 160$ is considered by the procedure to be too dense to liquefy.

Depth to ground water at most soundings was measured directly in the open hole created by the CPT. For soundings where measurements could not be made, it was inferred from a regional map of the water table prepared for this study. Depth to ground water was mapped primarily with water-level measurements in the holes created by the CPT soundings. These observations, however, were supplemented with water levels reported in boring logs that were collected by the California Geological Survey (CGS) as part of their preparation of regulatory seismic hazard zone maps of the area (see http://www.consrv.ca.gov/CGS/). Thus the resulting hazard map described here is based on average current or modern water levels.

To estimate the liquefaction hazard posed by each geologic unit for the M6.6 and 7.1 earthquakes on the Hayward Fault, LPI values were grouped by surficial geologic unit and cumulative frequency distributions of LPI were prepared (Figure 2). Although Halley and Graymer (1997) mapped subunits within the Holocene alluvial fan deposits, these subunits were not distinguishable with the CPT soundings and appeared to be geotechnically similar from a liquefaction potential perspective. Accordingly, LPI values computed for soundings in all of the subunits of the Holocene alluvial fan deposits were lumped together and assigned to a single geologic unit. Based on the calibration of LPI

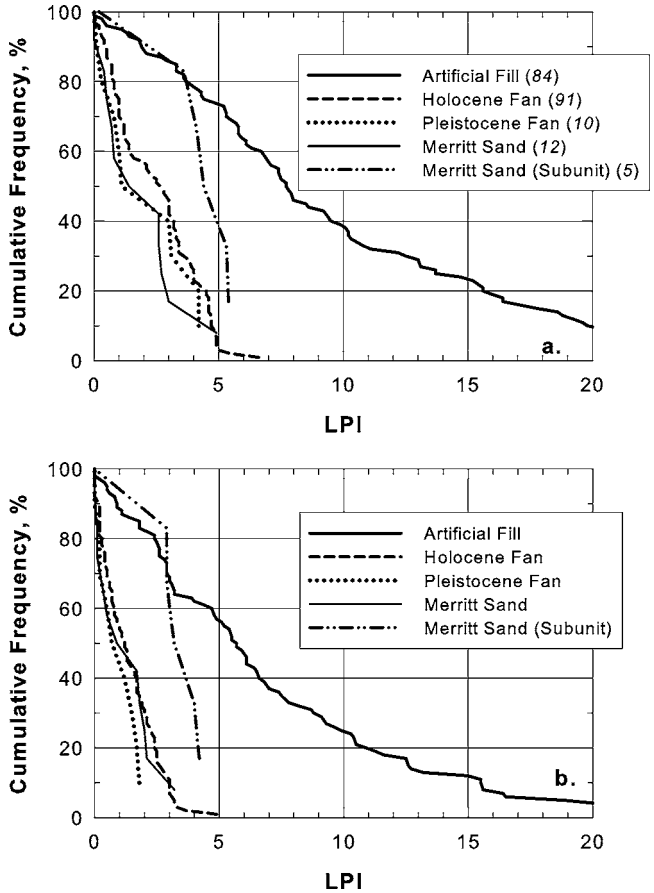


**Figure 2.** Cumulative frequency distributions of LPI for surficial geologic units in Alameda, Berkeley, Emeryville, Oakland, and Piedmont, California, for (a) M7.1 and (b) M6.6 earthquakes on the Hayward Fault. Number of CPT soundings conducted in each unit is shown in parentheses in legend of (a).

by Toprak and Holzer (2003) that surface manifestations of liquefaction in general occur where LPI $\geq$ 5, the percentage of soundings with LPI $\geq$ 5 for each geologic unit indicates the approximate percentage of surface area underlain by that unit that will exhibit surface manifestations of liquefaction. For the M7.1 earthquake, Figure 2a indicates that 73% and 3%, respectively, of the areas underlain by artificial fill and Holocene alluvial fan will exhibit surface manifestations of liquefaction. As will be discussed, approximately 38% of a portion of the area underlain by Merritt Sand is predicted to exhibit liquefaction effects (see the Merritt Sand (subunit) in Figure 2a). Surface manifestations of liquefaction are not anticipated for the areas underlain by the Pleistocene alluvial fan

deposits and most of the Merritt Sand because LPI $<5$. For the M6.6 earthquake, Figure 2b predicts that only the artificial fill will exhibit surface manifestations of liquefaction; 56% of the area underlain by the fill will be affected.

Although we have chosen to interpret the cumulative frequency at LPI $\geq 5$ as the percent area of the surficial geologic unit that is predicted to exhibit surface manifestations of liquefaction, we also believe that we could have interpreted it as the conditional probability of liquefaction at a given location. For example, we believe the prediction that 73% of the area underlain by artificial fill will liquefy during a M7.1 Hayward Fault earthquake also can be interpreted as a 0.73 probability that a randomly selected location underlain by fill will exhibit surface manifestations of liquefaction. Our choice of percent area rather than conditional probability was based on the primary intended audience for the maps: public officials and the general public. For engineering evaluations, probability may be more useful and preferred. As will be discussed later, interpreting the cumulative frequency at LPI $\geq 5$ as a conditional probability requires the assumption that the surficial geologic unit is spatially homogeneous.

The grouping of LPI by surficial geologic unit where units are less than 20 m thick ignores the contribution to LPI of underlying older geologic units in a given CPT sounding. Fortunately, within the present study area, liquefaction potential tends to be dominated by the mapped geologic unit exposed at the land surface, at least where the water table is in the surficial geologic unit.

## LIQUEFACTION HAZARD MAPS

The resulting liquefaction hazard maps for M7.1 and 6.6 earthquakes, respectively, on the Hayward Fault are shown in Figures 3 and 4. The maps are based on the cumulative frequency distributions of LPI shown in Figure 2. The maps indicate the percent area of each geologic unit that is predicted to exhibit surface manifestations of liquefaction for the specified earthquake scenario. Units without a demonstrable liquefaction hazard based on the LPI data, but which locally might have some hazard based on the seismic performance of similar age deposits elsewhere in the United States, were assigned to the $<1\%$ category. In addition to using mapped boundaries of geologic units to outline areas with different degrees of hazard, the area where the base of the Holocene alluvial fan deposits is above the water table was determined. Holocene alluvial fan deposits in this area do not contribute to the liquefaction hazard because the soil is dry. The liquefaction hazard derives from the deeper underlying Pleistocene alluvial fan deposits that are beneath the water table. To delineate the "hydrogeologic" boundary of this area, we mapped the thickness of Holocene alluvial fan deposits and computed the location of the line where the thickness equaled the depth to the water table using a geographic information system. The map of Holocene thickness was based on both USGS CPT soundings and borings in the CGS seismic hazard zone mapping database.

The liquefaction hazard of the Merritt Sand is not uniform in the study area. Three subareas with different degrees of hazard were recognized. Soundings in most of the area underlain by Merritt Sand yield LPI $<5$, which indicates the liquefaction hazard is negligible. However, soundings in the western part of northernmost exposure of Merritt

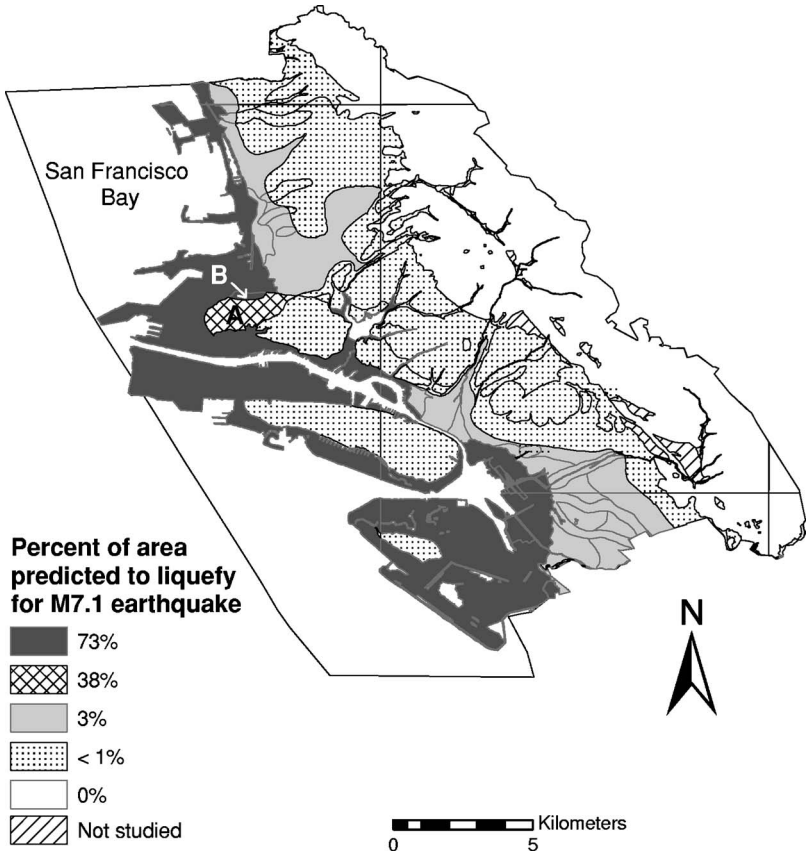


**Figure 3.** Liquefaction hazard map of Alameda, Berkeley, Emeryville, Oakland, and Piedmont, California, for a M7.1 earthquake on the Hayward Fault (modified from Holzer et al., 2002). Map shows areas where different percentages of the land area will exhibit surface manifestations of liquefaction. Areas A and B are sub-areas of the Merritt Sand with higher liquefaction potential. Estimates do not apply to local areas where soil has been improved.

Sand (see area A in Figure 3) yielded many LPI values greater than 5 for the M7.1 earthquake. Detailed exploration that included drilling and subsurface sampling revealed that this area is underlain by an approximately 1-m-thick laterally continuous layer of liquefiable sand (CPT tip resistance less than 5 $MN/m^2$) at a depth of about 5 m. Relief on the layer approximately follows surface topography. We believe the layer is the interface between the upper and lower members of the Merritt Sand identified by Trask and Rolston (1951). About 38% of the soundings yield $LPI \geq 5$ in this area for the M7.1 earthquake. In addition, along the northern boundary of this area, the upper part of the Merritt Sand is inferred from its low CPT tip resistance ($<5$ $MN/m^2$) to be loose (see area B in Figure 3). Soundings in area B yield $LPI \geq 10$ for the M7.1 earthquake. This area is south of a buried channel that was incised during the last low stand of sea level

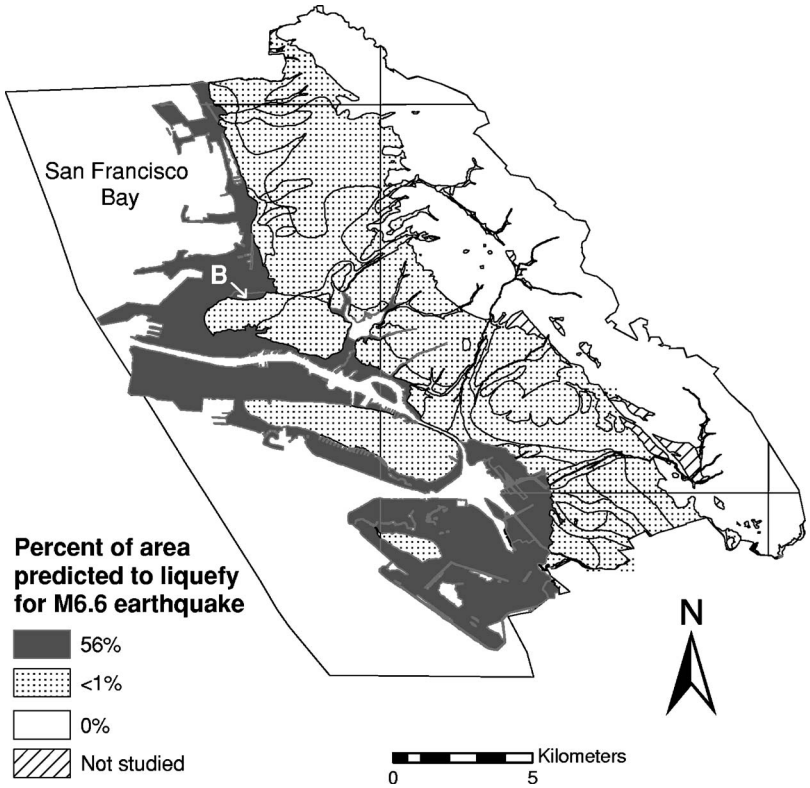


**Figure 4.** Liquefaction hazard map of Alameda, Berkeley, Emeryville, Oakland, and Piedmont, California, for an M.6.6 earthquake on the Hayward Fault. Map shows areas where different percentages of the land area will exhibit surface manifestations of liquefaction. Area B is a subarea of the Merritt Sand with higher liquefaction potential. Estimates do not apply to local areas where soil has been improved.

(see Holzer et al., 2005c, Figure 5a). Until the channel filled naturally with deposits during the last marine transgression, we speculate, on the basis of its nominal low relative density, that the Merritt Sand was reworked by surface runoff and landslides along the southern margin of the channel. The small area with LPI $\geq$ 10 was lumped together with the area underlain by artificial fill in the hazard map.

The liquefaction hazard in the area underlain by the 1-m-thick liquefiable layer in the Merritt Sand, area A, is reminiscent of subsurface conditions beneath the 1994 Balboa Boulevard lateral spread (Holzer et al. 1999). There, a 2.5-km$^2$ block of gently sloping ground slid along a 1- to 3-m-thick liquefied interval during the 1994 Northridge, California, M6.7 earthquake in an area where the topographic gradient was 1.6%. In area A in Oakland, the gradient approximately ranges from 0.4 to 1.6%. If the liquefiable layer in the Merritt Sand is indeed laterally continuous, it potentially could form a detachment surface similar to that at Balboa Boulevard.

The low ($<5$) LPI values for soundings in Pleistocene alluvial fan deposits and most of the Merritt Sand indicate that liquefaction of these two units during the scenario earthquakes is unlikely. Nevertheless, a small liquefaction hazard ($<1\%$) was assigned to the areas underlain by Pleistocene alluvial fan deposits and most of the Merritt Sand because liquefaction cannot be completely precluded at regional-scale hazard mapping. Regional mapping can overlook liquefiable soil in small areas if such soil is rare. The small estimated liquefaction hazard is consistent with historical performance of Pleistocene deposits during earthquakes in California, in which no liquefaction has been reported to date.

The liquefaction hazard map for the M7.1 Hayward Fault earthquake scenario is available in GIS format on-line at http://geopubs.wr.usgs.gov/open-file/of02-296/ (Holzer et al. 2002). The map also can be viewed in color at http://quake.usgs.gov/prepare/alameda.html.

## DISCUSSION

Cumulative frequency distributions of LPI of surficial geologic units offer a quantitative approach for regionally mapping liquefaction hazard because they can be used to estimate either how much area will be expected to show surface effects of liquefaction or the conditional probability of liquefaction at a specific location. The percentages of areas that are predicted to exhibit surface manifestations in the greater Oakland area are generally consistent with experience in recent earthquakes where similar deposits have been subjected to near-field ground motion. For example, the large percentage of the artificial fill that is predicted by this investigation to liquefy is consistent with the extensive liquefaction of loose fills during the 1995 earthquake in Kobe, Japan (Hamada et al. 1995). Similarly, the small, but nevertheless significant, area predicted to liquefy in areas underlain by Holocene alluvial fan deposits is consistent with observations following the 1994 Northridge, California, earthquake, where a small percentage of the alluvial fan deposits liquefied in the epicentral area in the San Fernando Valley (Holzer et al. 1999).

The minor hazard predicted for the Pleistocene alluvial fan deposits is consistent with the historical performance of Pleistocene deposits in California. As noted previously, liquefaction of Pleistocene deposits has not been reported in historical earthquakes in California. The prediction that 38% of part of the area underlain by Merritt Sand will liquefy is inconsistent with this performance. In fact, if only a slightly higher LPI threshold (e.g., $\mathrm{LPI} \geq 6$) had been applied, no liquefaction of the Merritt Sand would have been predicted. Deposits of Pleistocene age, however, have liquefied extensively in non-California U.S. earthquakes, notably the 1811/1812 New Madrid, Missouri, earthquakes and the 1886 Charleston, South Carolina, earthquake (Obermeier et al. 1990). Thus liquefaction of the Merritt Sand cannot be precluded on the basis of the late Pleistocene age of most of the unit. The liquefaction prediction is also seemingly inconsistent with the absence of reports of liquefaction during the 1906 San Francisco, California, earthquake. Lawson (1908, p. 302) surveyed damage in Oakland following the 1906 San Francisco, California, earthquake and did not report liquefaction in areas underlain by Merritt Sand. The absence of liquefaction in the Merritt Sand in Oakland in 1906, however, may be the result of lower ground shaking than that on which our pre-

diction for the nearby Hayward Fault M7.1 earthquake is based. For the 1906 M7.8 earthquake, which was on the San Andreas Fault about 20 km away from Oakland, we estimate a median PGA $\leq$ 0.3 g for sites underlain by the Merritt Sand (Boore et al. 1997). The PGA estimate was based on a $V_{S30}$=311 m/s for the Merritt Sand (Holzer et al. 2005a).

The one albeit modest test of the predictive capability of the methodology in the study area is the liquefaction of the artificial fill during the 1989 Loma Prieta (M6.9) earthquake. Based on 1:100,000-scale maps of liquefaction caused by the earthquake (Tinsley et al. 1998), approximately 13% of the area underlain by artificial fill showed surface manifestations of liquefaction. If a PGA of 0.2 g is assumed for this area, the cumulative frequency distribution of LPI predicts that 14% of the fill should have shown surface manifestations of liquefaction. Although recordings of ground motion at fill sites underlain by bay mud in the study area during the Loma Prieta earthquake are sparse, 0.2 g is consistent with those measurements. Mean PGAs of 0.14 and 0.28 g, respectively, were recorded at Treasure Island and Oakland Outer Harbor Wharf, both of which are underlain by younger bay mud (Borcherdt 1998). The real test of the LPI-based methodology for making liquefaction hazard maps, however, will be when the earthquake scenarios described here shake the study area. The liquefaction hazard maps serve as benchmark predictions of how the surficial geologic units in Oakland will respond to strong ground motion.

To evaluate the uncertainty of the liquefaction estimates for the two scenarios, we considered two sources of uncertainty: ground motion and the threshold value of LPI. For the two earthquake scenarios, we used the median PGA estimated with Boore et al. (1997) at an average distance of the study area from the Hayward Fault. Sixteenth-percentile (median minus one sigma) PGAs are 63% of the median values. For the M7.1 earthquake scenario, such a reduction in PGA reduces the predicted area of artificial fill that will be affected by liquefaction by a factor of approximately two. In addition, neither the Holocene alluvial fan deposits nor the Merritt Sand is predicted to liquefy. Thus uncertainty of the estimated ground motion has a significant impact on the predicted liquefaction area. For the threshold LPI value, we used the median value of 5 from Toprak and Holzer (2003). As noted earlier, their lower and upper quartile values for the threshold were 3 and 10. The predicted liquefaction is very different if these values are used as the threshold (see Figure 2). At a threshold value of 10 for both scenarios, only the artificial fill is predicted to show surface manifestations of liquefaction. For the M7.1 scenario, the percent area of the fills showing surface manifestations of liquefaction decreases from 73% to 39%. At a threshold value of 3, liquefaction is predicted to be extensive for both earthquake scenarios. For the M7.1 earthquake, all of the Pleistocene deposits are predicted to exhibit some surface manifestations of liquefaction including approximately 30% of Pleistocene alluvial fan deposits and 15% of the Merritt Sand. Approximately 40% of the Holocene alluvial fan deposit and 85% the subunit of the Merritt Sand are predicted to exhibit surface manifestations of liquefaction. These predictions of significant liquefaction of Pleistocene age deposits are inconsistent with historical experience in California as previously summarized. We suspect that the quartile values of Toprak and Holzer (2003) are more appropriately applied to measure the un-

certainty in the LPI prediction of a single CPT sounding. They do not appear to capture reasonably the uncertainty of the liquefaction threshold to be applied to cumulative frequency distributions. The uncertainty of the threshold to be applied to the cumulative frequency distributions should become clearer as liquefaction predictions based on these distributions are compared to observed areas of liquefactions in future earthquakes. The agreement between Iwasaki et al. (1982) and Toprak and Holzer (2003) of an LPI threshold of 5 suggests the uncertainty of the threshold value may not be large.

Finally, an important assumption in the use of surficial geologic maps to portray liquefaction hazard, which we adopted here with the exceptions of the Merritt Sand and the area where the base of the Holocene alluvial fan deposits was above the water table, is that each mapped geologic unit is spatially homogeneous. This clearly cannot be strictly true because thicknesses of units vary. Thus, to rigorously map liquefaction hazard, each mapped surficial unit should be further partitioned into subareas within which the unit is approximately homogeneous in terms of liquefaction susceptibility. While we recognize the desirability of such subdivision, it seldom will be practical because of the amount of subsurface information that is required. Nevertheless, we did visually inspect maps of LPI values in each surficial unit to confirm that they were spatially homogeneous to a first approximation. In fact, it was this inspection that led to subdividing the Merritt Sand. For the foreseeable future, we anticipate that geologic mapping will focus on distinguishing major surficial units, which in effect are subareas, using geologic criteria, and the fundamental challenge for hazard mapping will be to characterize the liquefaction susceptibility of each mapped surficial unit. Preparers of hazard maps, however, should be alert to situations where the assumption of spatial homogeneity is clearly invalid, as it was for the two exceptions noted here.

## ACKNOWLEDGMENTS

This investigation was partially supported by PG&E through a CRADA with the USGS. The maps for Berkeley and Oakland were prepared under the USGS and Federal Emergency Management Agency Project Impact Memorandum of Understanding. We thank Randall W. Jibson and Homa J. Lee of the USGS for reviewing the manuscript. We also thank Charles Real and the California Geological Survey for providing unpublished boring data and Selcuk Toprak for discussions during the development and preparation of the maps. Anonymous reviews by the *Earthquake Spectra* reviewers materially improved the manuscript.

## REFERENCES

Boore, D. M., Joyner, W. B., and Fumal, T. E., 1997. Empirical near-source attenuation relations for horizontal and vertical components of peak ground acceleration, peak ground velocity, and pseudo-absolute acceleration response spectra, *Seismol. Res. Lett.* **68** (1), 154–179.

Borcherdt, R. D. (Ed.), 1998. The Loma Prieta, California, earthquake of October 17, 1989—Strong ground motion, *U.S. Geol. Surv. Prof. Pap. 1551-A*, 272 pp.

California Division of Mines and Geology (CDMG, 1997. Guidelines for evaluating and mitigating seismic hazards in California, *Calif. Div. Mines and Geol. Spec. Pub. 117*, 74 pp.

Cetin, K. O., Seed, R. B., Der Kiureghian, A., Tokimatsu, K., Harder, L. F., Jr., Kayen, R. E., and Moss, R. E. S., 2004. Standard penetration test-based probabilistic and deterministic assessment of seismic soil liquefaction potential, *J. Geotech. Geoenviron. Eng.* **130** (12), 1314–1340.

Crespanelli, T., Madiai, C., and Vannucchi, G., 1999. Zoning for liquefaction risk in an Italian coastal town, in *Earthquake Geotechnical Engineering*, edited by P.S.S. Pinto, A. A. Balkema, Rotterdam, pp. 561–566.

Divakarla, P. K., Hoyos, L. R., Jr., and Macari, E. J., 1998. Assessment of liquefaction potential of western Puerto Rico, *Proceedings, Geotechnical Earthquake Engineering and Soil Dynamics III*, *Seattle*, pp. 530–541.

Frost, J. D., Carroll, D. P., and Rockaway, T. D., 1997. Spatial liquefaction analysis, in *Spatial Analysis in Soil Dynamics and Earthquake Engineering*, edited by J. D. Frost, ASCE Geotech. Spec. Pub. 67, pp. 70–86.

Hamada, M., Isoyama, R., and Wakamatsu, K., 1995. The 1995 Hyogoken-Nanbu (Kobe) earthquake—Liquefaction, ground displacement, and soil condition in the Hanshin area, The School of Science and Engineering, Waseda University, Tokyo, 194 pp.

Helley, E. J., and Graymer, R. W., 1997. Quaternary geology of Alameda County, and parts of Contra Costa, Santa Clara, San Mateo, San Francisco, Stanislaus, and San Joaquin counties, California: A digital database, *U.S. Geol. Surv. Open-File Rep. 97-97*.

Holzer, T. L., Bennett, M. J., Noce, T. E., Padovani, A. C., and Tinsley, J. C., III, 2002. Liquefaction hazard and shaking amplification maps of Alameda, Berkeley, Emeryville, Oakland, and Piedmont: A digital database, *U.S. Geol. Surv. Open-File Rep. 02-296.* http://geopubs.wr.usgs.gov/open-file/of02-296

Holzer, T. L., Bennett, M. J., Noce, T. E., and Tinsley, J. C., III, 2005a. Shear-wave velocity of surficial geologic sediments in Northern California: Statistical distributions and depth dependence, *Earthquake Spectra* **21** (1), 161–177.

Holzer, T. L., Bennett, M. J., Ponti, D. J., and Tinsley, J. C., III, 1999. Liquefaction and soil failure during the 1994 Northridge earthquake, *J. Geotech. Geoenviron. Eng.* **125**(6), 438–452.

Holzer, T. L., Noce, T. E., Bennett, M. J., Tinsley, J. C., III, and Rosenberg, L. I., 2004. Liquefaction-induced lateral spreading in Oceano, California, during the 2003 San Simeon Earthquake, *U.S. Geol. Surv. Open-File Rep. 2004-1269*. http://pubs.usgs.gov/of/2004/1269

Holzer, T. L., Noce, T. E., Bennett, M. J., Tinsley, J. C., III, and Rosenberg, L. I., 2005b. Liquefaction at Oceano, California, during the 2003 San Simeon Earthquake, *Bull. Seismol. Soc. Am.* **95** (6), in press.

Holzer, T. L., Padovani, A. C., Bennett, M. J., Noce, T. E., and Tinsley, J. C., III, 2005c. Mapping NEHRP $V_{S30}$ site classes, *Earthquake Spectra* **21** (2), 353–370.

Hosseini, S. M. M. M., 1998. Microzonation for liquefaction in Busehr, Iran, in *Proceedings, 11th European Conference on Earthquake Engineering, Paris*, pp. 1–9.

Iwasaki, T., Tatsuoka, F., Tokida, K.-i., and Yasuda, S., 1978. A practical method for assessing soil liquefaction potential based on case studies at various sites in Japan, in *Proceedings, 2nd International Conference on Microzonation, San Francisco*, pp. 885–896.

Iwasaki, T., Tokida, K., Tatsuoka, F., Watanabe, S., Yasuda, S., and Sato, H., 1982. Microzonation for soil liquefaction potential using simplified methods, *Proceedings, 3rd International Earthquake Microzonation Conference, Seattle*, pp. 1319–1330.

Lawson, A. C. (Chairman), 1908. *The California Earthquake of April 18, 1906, Report of the State Earthquake Investigation Commission*, Pub. No. 87, Carnegie Institution of Washington, Washington, D.C., Vol. 1, 192 pp.

Luna, R., and Frost, D. J., 1998. Spatial liquefaction analysis system, *J. Comput. Civ. Eng.* **12** (1), 48–56.

Obermeier, S. F., Jacobson, R., Smoot, J., Weems, R. E., Gohn, G. S., Monroe, J. E., and Powars, D. S., 1990. Earthquake-induced liquefaction features in the coastal setting of South Carolina and in the fluvial setting of the New Madrid seismic zone, *U.S. Geol. Surv. Prof. Paper 1504*, 44 pp.

Power, M. S., and Holzer, T. L., 1996. Liquefaction maps, *Applied Technology Council Tech-Brief 1*, 12 pp.

Robertson, P. K., 1990. Soil classification using the CPT, *Can. Geotech. J.* **27** (1), 151–158.

Robertson, P. K., and Wride, C. E., 1997. Cyclic liquefaction and its evaluation based on the SPT and CPT, *Proceedings, Evaluation of Liquefaction Resistance of Soils*, edited by T. L. Youd and I. M. Idriss, *National Center for Earthquake Engineering Research Tech. Rept. NCEER-97-0022*, pp. 41–87.

Seed, H. B., and Idriss, I. M., 1971. Simplified procedure for evaluating soil liquefaction potential, *J. Soil Mech. and Found. Div.* **97** (9), 1249–1273.

Seed, H. B., Tokimatsu, K., Harder, L. F., and Chung, R. M., 1985. Influence of SPT procedures in soil liquefaction resistance evaluations, *J. Geotech. Engrg.* **111** (12), 1425–1445.

Sonmez, H., 2003. Modification of the liquefaction potential index and liquefaction susceptibility mapping for a liquefaction-prone area (Inegol, Turkey), *Environ. Geol.* **44** (7), 862–871.

Sowers, J. M., 1993. Creek and watershed map of Oakland and Berkeley, Oakland Museum of California, Oakland, CA.

Tinsley, J. C., III, Egan, J. A., Kayen, R. E., Bennett, M. J., Kropp, A., and Holzer, T. L., 1998. Appendix: Maps and descriptions of liquefaction and associated effects, in The Loma Prieta, California, earthquake of October 17, 1989–Liquefaction, edited by T. L. Holzer, *U.S. Geol. Surv. Prof. Paper 1551-B*, B287-B314.

Toprak, S., and Holzer, T. L., 2003. Liquefaction potential index: Field assessment, *J. Geotech. Geoenviron. Eng.* **129** (4), 315–322.

Trask, P. D., and Rolston, J. W., 1951. Engineering geology of San Francisco Bay, California, *Geol. Soc. Am. Bull.* **62** (9), 1079–1110.

Ulusay, R., and Kuru, T., 2004. 1998 Adana-Ceyhan (Turkey) earthquake and a preliminary microzonation based on liquefaction potential for Ceyhan Town, *Natural Hazards* **32**(1), 59–88.

Working Group on California Earthquake Probabilities (WGCEP, 1999. Earthquake probabilities in the San Francisco Bay region 2000–2030: A summary of findings, *U.S. Geol. Surv. Open-File Rep. 99-517*, 36 pp.

———, 2003. Earthquake probabilities in the San Francisco Bay region 2002–2031: A summary of findings, *U.S. Geol. Surv. Open-File Rep. 03-214* (http://geopubs.wr.usgs.gov/open-file/of03-214).

Youd, T. L., and Hoose, S. N., 1977. Liquefaction susceptibility and geologic setting, in *Proceedings, 6th World Conference on Earthquake Engineering*, New Delhi, India, pp. 2189–2194.

Youd, T. L., and Idriss, I. M., Andrus, R. D. Arango, I., Castro, G., Christian, J. T., Dobry, R., Finn, W. D. L., Harder, L. F., Jr., Hynes, M. E., Ishihara, K., Koester, J. P., Liao, S. S. C., Marcuson, W. F., III, Martin, G. R., Mitchell, J. K., Moriwaki, Y., Power, M. S., Robertson, P. K., Seed, R. B., Stokoe, K. H., II, 2001. Liquefaction resistance of soils: Summary report from the 1996 NCEER and 1998 NCEER/NSF workshops on evaluation of liquefaction resistance of soils, *J. Geotech. Geoenviron. Eng.* **127** (10), 817–833.

(Received 14 April 2005; accepted 8 September 2005)